



Universiteit  
Leiden  
The Netherlands

## Photosynthetic Light Reactions at the Gold Interface

Kamran, M.

### Citation

Kamran, M. (2014, May 7). *Photosynthetic Light Reactions at the Gold Interface*. Casimir PhD series, Delft-Leiden. Retrieved from <https://hdl.handle.net/1887/25580>

Version: Not Applicable (or Unknown)

License: [Leiden University Non-exclusive license](#)

Downloaded from: <https://hdl.handle.net/1887/25580>

**Note:** To cite this publication please use the final published version (if applicable).

Cover Page



Universiteit Leiden



The handle <http://hdl.handle.net/1887/25580> holds various files of this Leiden University dissertation

**Author:** Kamran, Muhammad

**Title:** Photosynthetic light reactions at the gold interface

**Issue Date:** 2014-05-07

## **CHAPTER 4**

---

# **Role of co-factors in electron tunneling in bacterial RCs on a bare gold electrode**

# Abstract

In this chapter we examine the role of cofactors in electron tunneling in bacterial reaction center (RC) complexes between a gold surface and a conductive nanotip. In particular, we have studied an antenna-deficient strain of the photosynthetic bacterium *Rhodobacter sphaeroides* and two mutants, known as AM260W and AM149W, in terms of photo-activity and current-voltage characteristics by utilizing photoelectrochemistry and conductive atomic force microscopy (C-AFM). Using the Langmuir-Blodgett method to assemble monolayers of RC-membrane fragment we can obtain a dense packing, while the layer can be easily transferred to a gold electrode. These layers show a high degree of orientation, with the periplasmic side of the RC complexes facing the gold surface. Direct electron transfer from the gold surface to the special pair was observed, with a strongly asymmetric current response as function of the bias voltage. Electron tunneling by C-AFM is completely blocked in quinone-depleted reaction centers, while absence of the bacteriopheophytin in the so-called inactive branch has no effect. We conclude that electron tunneling as measured by C-AFM occurs exclusively along the A-branch of the reaction center.

## 4.1 Introduction

Photosynthesis is generally considered as the process used by plants and algae to sustain their metabolism and growth by utilizing solar energy. However, it is also found in a variety of bacterial systems, and the study of photosynthetic bacteria has provided a large part of our current understanding of light capture and energy transduction in photosynthesis. At the core of the photosynthetic reaction is the reaction center (RC) complex. It is a membrane bound pigment-protein complex where the primary reactions of photosynthesis take place. Solar energy absorbed by the antenna complexes is funneled to the RCs to initiate the charge separation leading to the generation of a transmembrane potential which is utilized to drive a series of reactions that are of physiological importance for the organism.

The bacterial RC is the simplest model system to study the basics of charge separation and energy conversion mechanisms in photosynthesis. A bacterial RC complex typically comprises three types of polypeptides, L, M and H, which together bind ten cofactors: four bacteriochlorophyll *a* molecules (a dimer P, plus two accessory bacteriochlorophyll molecules, B<sub>A</sub> and B<sub>B</sub>), two bacterio-pheophytines (H<sub>A</sub> and H<sub>B</sub>), two ubiquinones (Q<sub>A</sub> and Q<sub>B</sub>), a single carotenoid and a non-heme iron atom. The cofactors are arranged in more or less symmetrical branches A and B (hence the subscripts to denote the various cofactors).

The dimer of bacteriochlorophyll *a*, often termed the special pair, is located close to the periplasmic side of the membrane, whereas the non-heme iron is located close to the cytoplasmic side. The other cofactors are arranged in more or less symmetrical branches, A and B (hence the subscripts to denote the various cofactors). Despite the symmetry, these branches are found to be strongly asymmetric in terms of their functionality: the electron transfer path way is reported to be exclusively along the A-branch.<sup>1,2</sup>

The role of these cofactors is to initiate photosynthetic energy transduction by electron transfer across the membrane.<sup>3-5</sup> Light-induced electron transfer from the special pair (or primary donor) P to Q<sub>B</sub> is the key step of energy transduction. This electron transfer occurs in three steps involving subsequently the B<sub>A</sub>, H<sub>A</sub> and Q<sub>A</sub> cofactors, with the first steps happening on a picosecond time scale.

Although the bacterial RC has been extensively studied its functional asymmetry is still poorly understood. There are some studies showing the possibility of electron

transfer along the B-branch by introducing special mutations close to the primary donor site.<sup>6-13</sup> Up to 35-45% B-branch electron transfer is reported by using a quadruple mutant called LDHW, in which the reduction of H<sub>B</sub> is observed but the formation of P<sup>+</sup>Q<sub>B</sub><sup>-</sup> is not significant.<sup>6</sup> Apparently there is no functional role of the B branch of cofactors, although it is structurally very similar to the so-called active branch.

A key-aspect of the function of the reaction center is the tight packing of the cofactors. Indeed, it is this particular feature that accounts for the efficiency and quantum yield of light-induced, primary charge separation. The RC can be viewed as a natural, nanoscale device with characteristics that are very much sought after in molecular electronics. From this point of view it is of interest to examine the coupling of reaction center complexes with conductive metal contacts. A key question here is the possibility of electron exchange with electronic circuit elements, and in particular how the system responds to the injection of electrons from a connected electrode. To address this question we have investigated the properties of photosynthetic RCs by conductive atomic force microscopy (C-AFM), where membrane-embedded RCs were adsorbed on a flat gold electrode, and probed by a gold-coated AFM tip approaching from the opposite side. C-AFM is a very important technique to study electronic properties of materials down to the molecular level. It has been previously utilized to study organic molecules including photosynthetic pigment-protein complexes<sup>14-20</sup>.

For this work we have used chromatophores from a RC-only mutant from *Rhodobacter (Rb.) sphaeroides*. Further details were obtained by examining the AM149W and AM260W variants, two well-known mutants of this antenna-deficient strain of *Rb. sphaeroides*. Mutation of residue Ala 149 to Trp in the M-subunit of the RC (AM149W) results in the formation of RC complexes without H<sub>B</sub>. The other mutant, AM260W, is the result of an Ala 260 to Trp mutation; this mutant RC lacks the Q<sub>A</sub> cofactor.<sup>21-24</sup> These two mutants have been previously studied by utilizing x-ray crystallography<sup>21,24</sup>, EPR<sup>6,13</sup> and other spectroscopic techniques.<sup>7,8,25,26</sup>

Apart from C-AFM we have also employed photoelectrochemistry techniques to measure the photoactivity of these complexes and the consequences of the removal of the cofactors. By measuring photocurrent generation by membrane-embedded,

native RCs and of the AM149W and AM260W mutants, along with current-voltage spectroscopy of these complexes, the role of the co-factors in trans-membrane electron transfer can be evaluated.

Our results indicate that membranes containing RCs attached to bare gold electrode are photoactive and support substantial photocurrents in both directions that is from RCs to electrode and *vice versa* depending on the orientation of the RCs and the polarity of applied electric potentials.  $Q_A$  is shown to have a very important role in the electronic communication between the electrodes across the membranes, whereas a missing  $H_B$  cofactor does not have any effect on the performance of the mutant RC in comparison with the native complex. The current-voltage spectroscopy measurements support the findings of photocurrent experiments. Our results show that electron injection from the electrode gives rise to charge transfer exclusively along the A branch of the RC, similar to the process that results from optical excitation of the primary donor.

## 4.2 Materials and methods

### RCs containing membranes and mutants

Antenna deficient membranes and mutants AM260W and AM149W were prepared and cultured according to previously described protocols.<sup>22,24,25</sup> These mutations were applied to the *Rb. sphaeroides* deletion strain DD13, utilizing a quick-change mutagenesis kit (from Stratagene). The antenna-deficient strains of *Rb. sphaeroides* was grown under semi-aerobic conditions in the dark. Harvested cells were re-suspended in 10 mM Tris buffer (pH 8) and broken by using a French press (Arminco). Membranes were purified by ultracentrifugation at 4 °C and 27,000 rpm in a TY45 rotor for 4 hours using a sucrose step gradient (15-40%). Membranes were concentrated by ultracentrifugation and stored at -20 °C.<sup>22,24,25</sup>

### Working electrode preparation

Working electrodes for photocurrent measurements were prepared by sputtering a gold film on glass cover slips. Before gold deposition, the glass cover slips were cleaned by sonication in methanol for one hour, subsequently rinsed with milli-Q water and then dried in a stream of nitrogen gas. Before gold deposition, the cleaned cover slips were placed in an ozone cleaner (UVP PR-100, UV-ozone Photoreactor) for one hour.

## **Gold deposition**

A thin layer of gold was sputtered on clean glass cover slips by utilizing a magnetron sputtering system (ATC 1800-F from AJA Corporation).<sup>27</sup> In order to improve the adhesion between the glass surface and the gold layer, a thin layer (1-2 nm) of molybdenum-germanium (MoGe) was sputtered first on the glass surface. The gold film of 12 nm thickness was then sputtered on top of it. The sputtering rate for MoGe was 1.32 nm/min in a 10 mTorr Argon environment, whereas the gold was deposited at a rate of 9.06 nm/min in a mixture of 10 mTorr Argon and 1 mTorr oxygen. The gold layers we thus obtained were flat (about 2-3 Å root-mean-square roughness), homogenous and conductive over the full area of the coating. Gold-coated glass cover slips were stored in a desiccator, and used within one week after preparation.

## **Langmuir Blodgett deposition**

The Langmuir Blodgett (LB) technique was used for deposition of RC-only membrane fragments for IV spectroscopy. The solution of membrane fragments (1 mg/mL) was spread on the surface of water in a LB trough, and after equilibration the surface assembled, RC-containing membranes were compressed to a surface pressure of 35 mN/m. A gold-coated glass cover slip with a diameter of 25 mm was vertically dipped into the sub phase at a speed of 1mm/min. The surface pressure was kept constant during this procedure.

## **Adsorption of RC-membranes on gold electrode from solution**

As an alternative to LB deposition, RC-containing membranes were adsorbed on a gold surface by incubating the gold-coated glass cover slips into the solution of RC-membranes for one hour at 4 °C. The gold surface was then rinsed with buffer (Tris-HCl pH 8) to remove the loosely and non-bound membrane fragments.

## **Photocurrent measurement**

Photocurrents generated by bacterial RCs were measured by using a conventional three-electrode setup. The reference electrode (saturated calomel electrode) and counter electrode (platinum wire) were inserted into a homemade measuring cell containing Tris buffer (pH 8) as measuring solution. A gold-sputtered glass slide (25 mm diameter) was incorporated as the base of the cell, and served as the working electrode. Illumination was provided by a light emitting diode (LED) with a central wavelength of 880 nm and a bandwidth of 50 nm. A computer controlled

shutter was placed between the light source and measuring cell to turn the light illumination on or off. The LED was operated at 800 mA and 7.6 V. The intensity of light reaching the surface of the working electrode was 23 mW/cm<sup>2</sup>. In order to record action spectra, a white light source equipped with a monochromator was used as the light source. The light intensity at the surface of the working electrode in this case was 2 mW/cm<sup>2</sup> at 880 nm. The wavelength of the light was increased in steps of 5 nm and light illumination was turned on for 10 seconds at every wavelength. Ubiquinone-0 and cytochrome *c* were used as redox mediators in the solution for charge transportation to the counter electrode.

### **Absorption spectra of RC-membranes adsorbed on a gold electrode**

In order to estimate the surface coverage of mutants of RC-membranes, we measured the absorption spectra of the RC-membrane/gold-coated cover slips. The spectra were recorded by using a fiber-coupled spectrometer (Ocean Optics, HUV4000) equipped with a CCD array detector, and with halogen and deuterium lamps as light sources.

### **Atomic force Microscopy (AFM)**

The topography of membrane-embedded bacterial RCs deposited on a gold electrode was checked by using AFM (Nanoscope IIIa, Veeco, USA) in tapping mode under ambient conditions. Standard silicon nitride cantilevers with resonant frequency of 75 kHz and force constant of 2 N/m were used for imaging.

### **Conductive atomic force Microscopy (C-AFM)**

Current-voltage characteristics of surface-adsorbed RC membrane fragments were measured by C-AFM. The junction was fabricated by sandwiching the RC complexes between the C-AFM tip and the gold surface. Unlike normal AFM, a conductive probe is required for I-V spectroscopy. Therefore, standard silicon nitride probes were coated with a thin layer of platinum by using a magnetron sputtering system (ATC 1800-F from AJA Corporation). The radius of curvature of the probe after sputtering was about 15 nm (checked by scanning electron microscopy). Tapping mode AFM imaging was used to locate the RC complexes, after which the tip was positioned on top of it with control of the applied force. A voltage ramp was applied between the tip and substrate and the resulting current was measured. The current-to-voltage converter, mounted very close to the C-AFM tip, limited the current measurements to values of less than  $\pm 10$  nA.

### 4.3 Results

It was shown by Magis et al. that membrane fragments isolated from *Rb. sphaeroides* can be adsorbed on a bare gold surface while retaining their functional properties. Moreover, they adsorbed strong enough that the fragments were not removed by gentle rinsing and drying. We followed similar procedures to adsorb RC-only membrane fragments from wild-type and mutants of *Rb. sphaeroides* on a semi-transparent, bare gold surface. For this purpose, gold-coated cover slips were incubated for one hour at 4 °C with a solution of the RC-only membrane fragments (see materials and methods). After rinsing with buffer solution, we measured the absorption spectra of the adsorbed layers, which are shown in figure 1. From the extinction coefficient at 803 nm ( $288 \text{ mM}^{-1}\text{cm}^{-1}$ ).<sup>28</sup> we calculate that the surface is covered by about  $2.7 \times 10^{12}$  RC-complexes per  $\text{cm}^2$ . Based on the dimensions of the RC complex<sup>29</sup>, we estimate that this corresponds to about 60-70% of a full mono-layer if we assume a close packing.

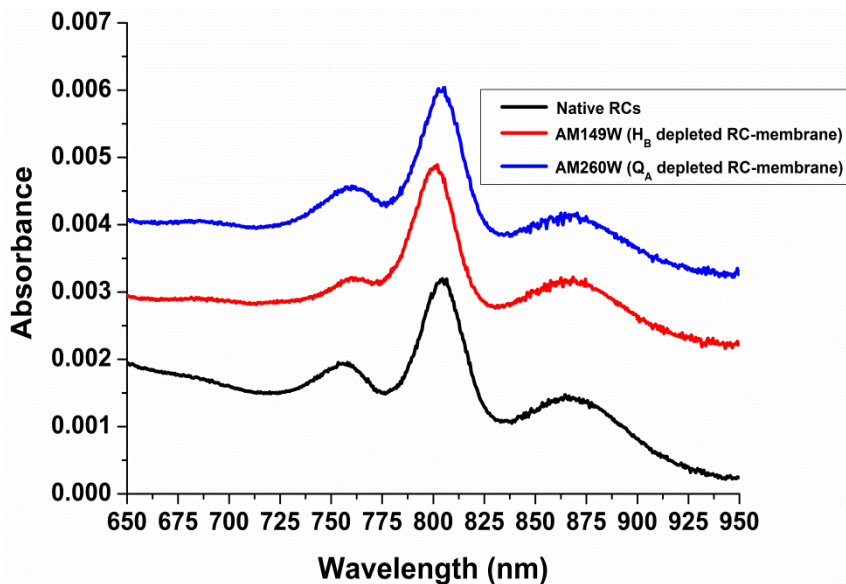
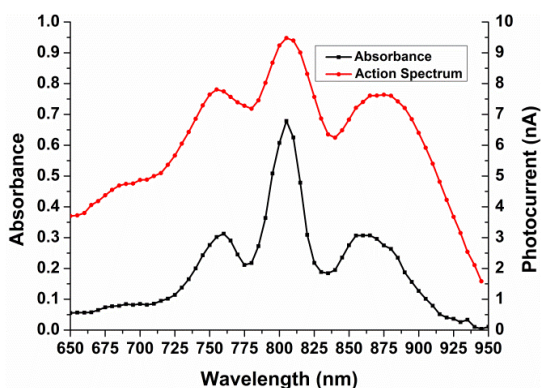


Figure 1. Absorption spectra of layers of membranes fragments containing either native RCs of *Rb. sphaeroides*, or variant RCs with missing cofactors. The absorption spectra were recorded after incubating the gold-coated cover slip for one hour with chromatophores and subsequent rinsing with buffer (Tris pH 8) to remove loosely or non-bound material. Black curve: Membranes containing native RCs; red curve: with  $H_B$ -depleted RCs; blue curve: with  $Q_A$ -depleted RCs.

The absorption spectra show that the native RCs fragments, the AM149W and the AM260W variants adsorb equally well on the gold surface. The lower amplitude of the 760 nm band in the absorption spectrum of the AM149W variant confirms the depletion of the H<sub>B</sub> cofactor. Below we will first discuss the results that were obtained with membrane fragments containing native RCs, after which we turn to data of the RC variants from the AM149W and AM260W mutants of *Rb. sphaeroides*.

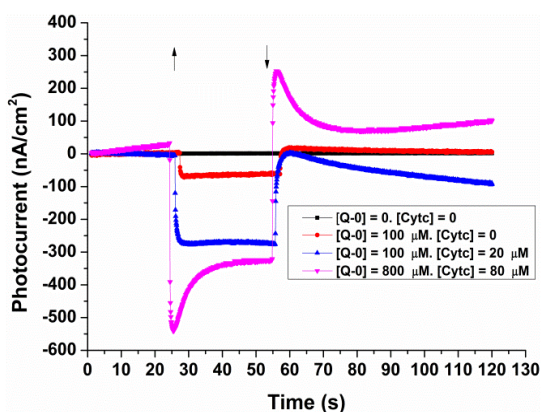
### 4.3.1 Monolayers of membrane fragments containing native RCs

For photocurrent measurements the RC-functionalized gold-coated cover slip was incorporated in an electrochemical cell. This cell was configured in a conventional three-electrode configuration with the gold-coated cover slip as the working electrode at the base. The reference (saturated calomel) and counter (platinum wire) electrodes were inserted in the buffer solution (Tris pH 8) that filled the cell. This buffer solution also contained mediators, in particular ubiquinone-0 (Q-0) and



**Figure 2**

(A) Absorbance spectrum (black curve) and action spectrum (red curve) of native RCs adsorbed on bare gold electrode. The wavelength of the light was increased in steps of 5nm by using a monochromator, and the photocurrent was recorded at each wavelength by turning the light illumination on for 10 seconds.



(B) Photocurrents generated by native RC-containing membranes at different mediator concentrations. Without mediators no photocurrent was recorded (black squares), with 100 μM of Q-0 a small photocurrent was observed (red squares) which increased with the addition of 20 μM of cyt c (blue triangles). The highest photocurrent (peak value) was recorded at 800 μM of Q-0 and 80 μM of cyt c.

cytochrome (cyt) *c*. The electrodes were connected to a potentiostat, and the sample could be illuminated from the bottom of the cell, through the gold layer.

In order to verify that the source of the photocurrent is the charge separation in the RC we recorded the action spectrum, i.e., the photocurrent as a function of the excitation wavelength in the presence of Q-0 and cyt *c*. The mediators assist in shuttling electrons from the Q<sub>B</sub> site to the counter electrode and from the working electrode to the special pair, respectively. The results for native RCs in figure 2a show that the action spectrum (red curve) follows the absorption spectrum (black curve). The action spectrum is broadened by the 40 nm bandwidth of excitation, which is about an order of magnitude larger than that of the absorption spectrum.

The effect of the mediators is apparent from figure 2B. Here we show the photocurrent response of native RC-containing membrane fragments as a function of time when the light (from a light-emitting diode operating at 850 nm) is switched on for a time interval of a few tens of seconds. The measurements were performed at an applied potential of  $-100$  mV vs SCE. We did not observe any photocurrent in the absence of both mediators (Fig. 2B, black data points). When only Q-0 is present in the measuring solution a photocurrent of about  $50$  nA/cm<sup>2</sup> is recorded (red data points). The photocurrent increases substantially, to  $350$  nA/cm<sup>2</sup>, when the measuring solution is supplemented with  $20$  μM of cyt *c*. The photocurrent depends on the concentration of mediators. The highest photocurrent, a peak value of  $550$  nA/cm<sup>2</sup>, was obtained when the measuring solution contained  $800$  μM of Q-0 and  $80$  μM of cyt *c*. At these high concentrations the photocurrent response shows a transient component.

Figure 3A shows the photocurrent response as a function of applied potential in the range of  $-175$  to  $+175$  mV in steps of  $25$  mV in the presence of, both, Q-0 ( $800$  μM) and cyt *c* ( $80$  μM) as mediators in the solution. The magnitude of the photocurrent increases sharply with increasingly negative potentials. The highest photocurrent is recorded at  $-125$  mV vs SCE. At positive potentials the photocurrent has the opposite direction of that at negative potentials, although much lower in amplitude. This is likely due to a distribution of opposite orientations of the RC-membrane fragments on the gold surface. The difference in amplitude may be indicative of preferred orientations, but the effectivity of the mediators may also vary from one orientation to the other.

The RC-generated photocurrents are also dependent on the intensity of light illumination. The intensity dependence is shown in figure 3B. The photocurrent was found to be linear over the range of intensities that was available.

Although the adsorbed RC-containing membrane fragments on a gold surface appears to form a rather dense layer, the orientation of the fragments cannot be easily controlled or ascertained. It is known that Langmuir Blodgett (LB) techniques can be used to form mono-layers of RC complexes and of RC-containing membrane fragments at the air-water interface.<sup>30-34</sup> This method offers more control over experimental parameters than adsorption from solution. For this reason we explored the use of LB techniques to transfer mono-layers of RC-membrane fragments to a gold-coated glass slide. A solution of membranes fragments (1 mg/mL) was spread on the water sub-phase in a LB trough. After equilibration, the surface assembled membranes were compressed by the barriers of the LB trough up to a surface pressure of 35 mN/m. This surface pressure was

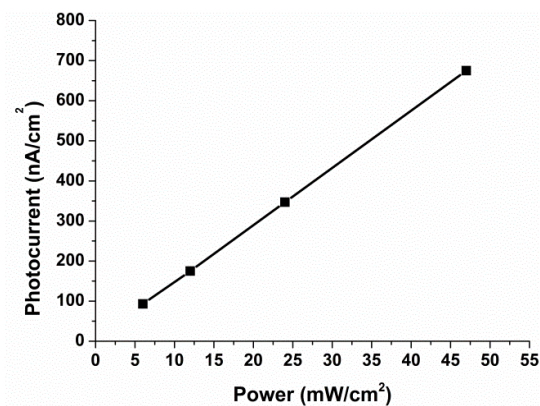
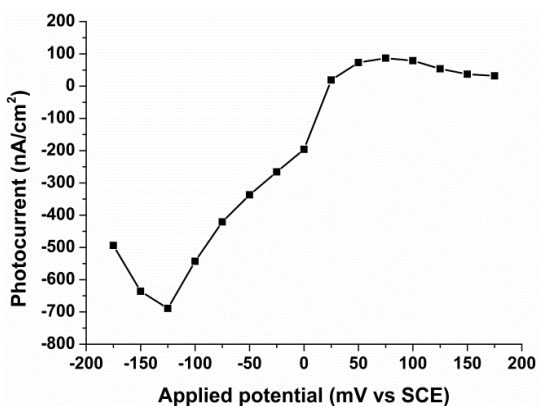


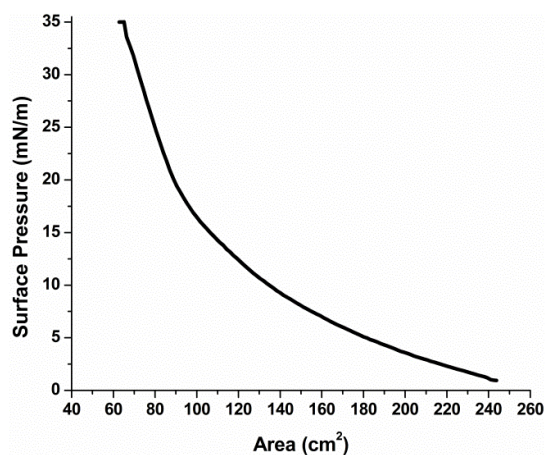
**Figure 3**

(A) The photocurrent response of RC-containing membrane fragments adsorbed on a bare gold electrode at different applied potentials. The measuring solution 800  $\mu\text{M}$  of Q-0 and 80  $\mu\text{M}$  of cyt *c* as charge carriers. The potential was varied from  $-175\text{mV}$  to  $+175\text{mV}$  (vs. SCE) in steps of 25 mV.

(B) Photocurrent response of RC-containing membrane fragments adsorbed on a bare gold electrode as a function of light intensity at a potential of  $-125\text{ mV}$  (vs SCE). The measuring solution also contained 800  $\mu\text{M}$  of Q-0 and 80  $\mu\text{M}$  of cyt *c* as redox mediators.

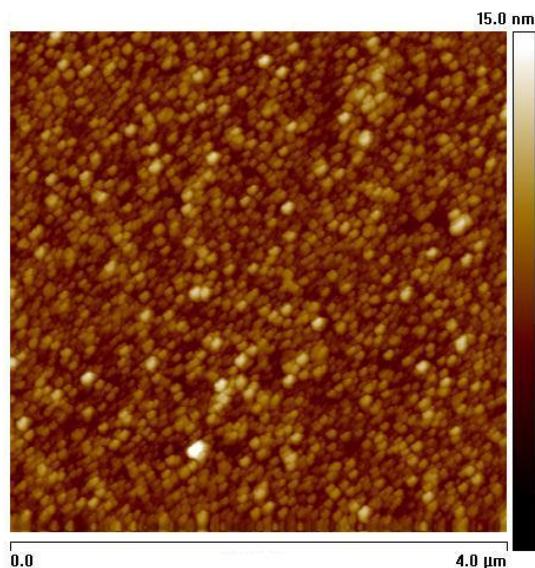
chosen to avoid any structural deformation induced by the deposition process. A gold coated glass slide was dipped in at a speed of 1 mm/min, keeping the surface pressure constant; the slide was then pulled out at the highest available speed to avoid any deposition during this step.

Figure 4A shows the characteristic compression curve of RC-membrane fragments spread on the water surface in the LB trough. Upon compression of the surface-assembled membrane fragments, the surface pressure rises gradually with an increasing slope. After transfer of the monolayer to a gold-coated cover slip we measured the surface topography by atomic force microscopy (AFM) in tapping



**Figure 4:**

(A) Compression curve of a layer of RC-containing membrane fragments on the water-air interface of a Langmuir-Blodgett (LB) trough. Compression was performed by moving the barriers at a rate of 5 mm/min up to a surface pressure of 35 mN/m.

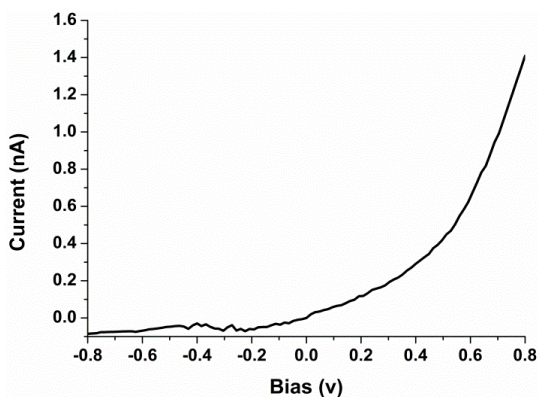


(B) Atomic force microscopy (AFM) image of a layer of RC-containing membrane fragments deposited by the LB method. The topograph was obtained by using tapping mode AFM under ambient conditions. Standard silicon nitride cantilevers were used for imaging, with a spring constant of 2.8 N/m and a resonant frequency of 75 kHz.

mode. The AFM image (Figure 4B) shows closely packed membrane fragments with a fairly uniform height distribution.

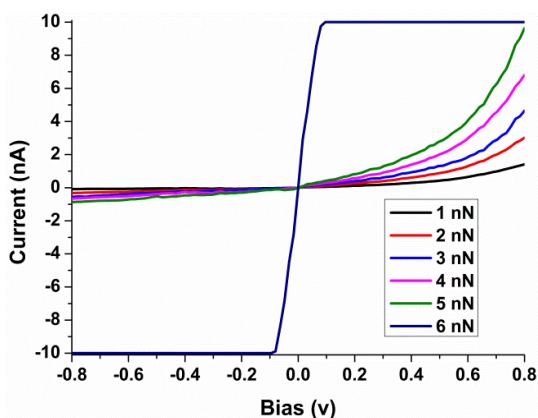
The interaction between the monolayer and the underlying electrode was investigated by current sensing AFM, similarly as described in Chapter 2. Current-voltage curves were measured across the of LB film of native RC-containing membranes fragments in the tunneling junction formed by the conductive AFM tip and the gold substrate. The cantilever of the AFM used in this case was made of silicon nitride, coated with a thin layer of platinum. The contact force exerted by the probe tip was controlled by AFM feedback in contact mode.

Figure 5A shows a typical I-V curve of (native) RC-containing membranes deposited on a gold electrode, at an applied force of 1 nN. The I-V curve has a pronounced asymmetry, with a small to negligible current at negative potentials, whereas at increasing positive potentials a nonlinear rise of the tunneling current is



**Figure 5:**

(A) Typical current-voltage curve of a RC-containing membrane fragment in a LB-deposited layer on a flat gold electrode. The layer is sandwiched between the gold electrode and a conductive AFM tip. The applied force in this case is 1 nN.



(B) Current-voltage curves of RCs containing membranes sandwiched between the electrode and AFM tip. A membrane patch was located by tapping mode AFM, the instrument was then switched to contact mode and a voltage ramp was applied between the tip and substrate to record the resulting current. Current-voltage curves were recorded as a function of contact force.

observed. The shape of the curve has the characteristics of a diode junction. The current reaches a value of 1.4 nA at a bias voltage of 0.8 V and a contact force of 1 nN. In Chapter 1 we described a similar asymmetry in the I-V curves of RC-LH1 complexes, although this component was superposed on the contribution of the LH1 complex to the tunneling current. The present experiments confirm the interpretation of this asymmetric component as arising from the RC complex within the LH1 ring. The dependence of the tunneling current on the force exerted on the RC-membrane layer by the tip is shown in Figure 5B, showing an increase of the tunneling current with the applied force. The trend is very similar to that of the asymmetric component in the data shown in Chapter 1 for the 2D-crystals of RC-LH1. Also in the present case we observe a breakdown of the monolayer at higher force, although the breakdown force of about 6 nN is significantly lower than for the 2D RC-LH1 crystals.

### 4.3.2 Monolayers of RC-variants.

The AM149W and AM260W RC variants each lack a specific cofactor: the AM149W variant does not contain H<sub>B</sub>, while the AM260W variant lacks Q<sub>A</sub>. (For details of the cofactor composition and arrangement we refer to Chapter 1 of this thesis). We first consider the photocurrent response of surface assembled membrane fragments with these two variants in comparison with that of native RC-containing fragments.

The photocurrent response of native RCs, AM149W and AM260W is shown in Figure 6a. Photocurrents were measured at a potential of -100mV (*vs* SCE), using in all cases the same concentration of Q-0 (800 μM) and cyt *c* (80 μM) and the same light intensity (23 mW/cm<sup>2</sup>, centered at 850 nm, measured at the electrode surface). We also note that the surface density of the RCs in all three cases was very similar, as concluded (and calculated) from the absorption spectra shown in figure 1. Despite very similar measurement conditions, the photocurrent response of the complexes was different. The magnitude of the photocurrent from native RCs membranes and the AM149W variant was very similar, reaching a (peak) value of 550 nA/cm<sup>2</sup>. In the case of the AM260W variant, however, a very different response was observed: in fact no photocurrent was recorded upon light illumination of this particular RC variant.

Current-voltage curves of all three RC-variants were recorded under the same conditions. Figure 6B shows the I-V curves of AM149W, AM260W and native RC-containing membrane fragments deposited on a gold electrode by transfer of the LB monolayer formed at the air-water interface. All the samples were prepared with the same compression rate and surface pressure, and the I-V curves were recorded at the same contact force of 1 nN. The native RC and the AM149W RC-variant have strikingly similar I-V characteristics, whereas AM260W has a completely different character as measured by conductive AFM. The magnitude of the tunneling current for native RCs reached values of 1.3 to 1.4 nA for AM149W at a bias voltage of 0.8 V but no current was recorded for the AM260W variant.

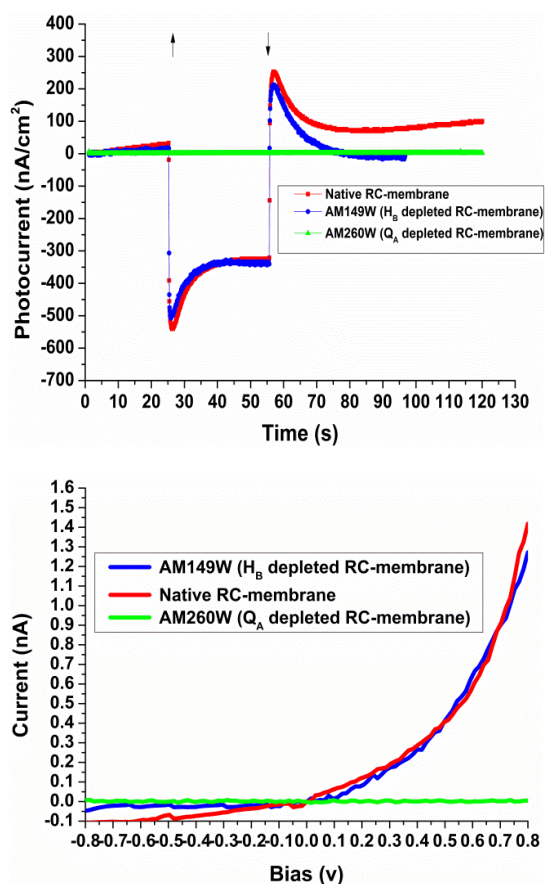


**Figure 6.**

(A) Photocurrent RC-containing membrane fragments on gold at a potential of  $-100$  mV (vs SCE), containing, respectively, native RCs (red squares),  $H_B$ -depleted RCs (blue circles) and  $Q_A$ -depleted RCs (green triangles).  $Q_0$  ( $800 \mu\text{M}$ ) and  $\text{cyt } c$  ( $80 \mu\text{M}$ ) were used as redox mediators. Light intensity at the surface was  $23 \text{ mW}/\text{cm}^2$ . Up/down arrows indicate light being switched on/off

(B) IV-spectroscopy of membrane bound native RCs complexes and mutants with missing cofactors. IV curves of membrane-bound native RCs and mutants were recorded by using conductive AFM in contact mode. I-V curves were recorded at an applied force of 1 nN.

## 5. Discussion

Bacterial RCs have been previously deposited on electrodes by using various immobilization techniques, including adsorption on functionalized electrodes, genetically modified complexes attached to the surface via linker molecules, Langmuir Blodgett deposition and RCs entrapped in porous material etc.<sup>17,35-41</sup> An often used approach to assemble photosynthetic pigment complexes on an electrode or other functional surface is based on an engineered coupling between the complex and the surface, for example by using an interfacial layer or specific molecular linkers.<sup>15,38-40</sup> It is usually assumed that it provides an effective way to control the orientation of the protein complex which is important because of the vectorial character of photosynthetic electron transfer. The results in this chapters show that a bare gold electrode also provides a surface for relatively stable adsorption of photosynthetic pigment-protein complexes, that a high surface density can be achieved by simple methods, and that a high degree of orientation can be obtained.

We observed that simple adsorption from solution results in a high surface density of adsorbed RC-complexes on a gold surface. The functionality and activity of the immobilized RCs was verified by measuring the light-induced action spectra of the photocurrent in an electrochemical cell. Since the RC-complexes are adsorbed on the working electrode it is essential to have a mediator in the solution to facilitate electron transport to or from the counter electrode. Optical excitation of the primary donor P in the RC results in reduction of  $Q_A$  and subsequently  $Q_B$ . In nature, the reduced  $Q_B$  can be exchanged and replaced by a member of the quinone pool in the photosynthetic membrane. In the experiments described in this chapter, we have Q-0 in solution, and we conclude that it plays a similar role as the quinone pool in nature by accepting electrons from  $Q_A$ , after which it is oxidized at the counter electrode. This is supported by the observation of a photocurrent when only Q-0 is present as mediator, which is in the oxidized form at a potential around -100 mV. It also implies that under those conditions direct electron transfer takes place from the working electrode to the primary donor, at least in a significant fraction of the RC complexes. We stress this last point, because it is quite possible that not all RC complexes were properly oriented on or in sufficiently close proximity to the gold surface for direct electron transfer.

Indeed, we do observe a significant increase of the photocurrent when a second mediator, *cyt c*, is added to the solution. At negative potentials *cyt c* is in the reduced state, and capable of electron transfer to the photo-oxidized primary donor, similarly as in nature. This suggests that *cyt c* assists in the electron transfer from the working electrode to the primary donor. This is consistent with the results of earlier studies<sup>42,43</sup> which showed that *cyt c* binds in a more or less stable form to gold-adsorbed RC-complexes. It is not clear how such a construct is arranged, but probably *cyt c* becomes inserted in the free space between or near RC complexes and the gold surface. The stability of such a construct could be the result of the interaction of *cyt c* with exposed functional groups of the RC complex or the lipid molecules on one hand and with the gold surface on the other hand. Some support for this conjecture comes from a study of the gold substrate topography on the voltammetry of *cyt c* adsorbed on self-assembled monolayers (SAMs), showing that surface roughness and SAM defects significantly increased *cyt c* adsorption and the effectiveness of electronic coupling.<sup>44</sup>

The magnitude of the photocurrent depends on the concentration of two mediators. It increased with the concentration of, both, Q-0 and *cyt c*, but eventually the increase levels off. The photocurrent became saturated when the Q-0 and *cyt c* concentrations reached 800  $\mu\text{M}$  and 80  $\mu\text{M}$ , respectively. When the concentration of the mediators was increased the time profile of the photocurrent changed during and following the light on interval. At higher concentrations a transient component was observed, both, when the light was switched on and switched off. The amplitude of these components also increased with increasing mediator concentration. When the light is switched on, the instantaneous photocurrent decays to a more or less steady level at a time scale of seconds. The transient that follows after the light is switched off has a similar shape and amplitude, but an opposite sign. These transients can be attributed to storage of charge in the Q-0 pool in solution, which becomes partially reduced because of diffusion limitations. The electron transfer rate will follow the equilibration of the charge distribution after the light is switched on. The reverse transient is probably due to charge recombination when the light is switched off.

The RC-generated photocurrent is also dependent on the applied potentials. At negative potentials a much higher photocurrent is recorded compared to positive potentials, while the current has opposite directions. For negative potentials the

photocurrent is generated by electron flow from the working electrode to the photo-oxidized primary donor in the reaction center. Direct electron transfer requires a close proximity of the primary donor to the gold surface, which suggests that the contribution to the photocurrent is primarily from RCs that are oriented with the periplasmic side towards the electrode. From the photocurrent measurements, however, we cannot determine the fraction of RCs that are in this favorable orientation. Possibly the reversal of the photocurrent at positive potentials is due to differently oriented RCs. Photocurrents generated by RCs with different orientations have also been reported in literature, where the desired orientation was achieved by using linker molecule between genetically modified protein complexes and the electrode. Higher photocurrents were recorded in these experiments when the periplasmic side of the RCs was facing the working electrode, compared to the opposite orientation. The difference in electron transfer rate was attributed to the larger tunneling distance when the H subunit is oriented towards the electrode.<sup>39</sup>

The maximum current response is observed around a potential of  $-125$  mV vs. SCE. This is consistent with the redox properties of the mediators. Cyt *c* has a midpoint potential of  $11$  mV vs SCE and is almost fully reduced at a potential of  $-125$  mV. The redox chemistry of ubiquinones, however, is less straightforward, involving one or two reduction steps and different protonation states. No less than 9 different redox and protonation states can be identified.<sup>45</sup> For this discussion, the most important step is the one-electron reduction of the  $Q_A Q_B$  pair in the RC. Gunner *et al.* have calculated that the corresponding reduction potentials for the formation of  $Q_A^- Q_B$  and  $Q_A Q_B^-$  are, respectively,  $-271$  and  $-251$  mV vs. SCE.<sup>45</sup> The reduction potential of the  $UQ-0/UQ-0^-$  couple in solution is expected to be more positive than it would be in the  $Q_B$  site of the RC, if only for the higher dielectric constant in solution. Thus there is roughly a window of  $-200$  to  $0$  mV where the two mediators can be effective to sustain a photocurrent in a properly configured cell.

The photocurrent measurements do not provide conclusive information about the orientation of the RCs on the electrode surface, although a sizable fraction of the RCs must be in a favorable orientation. It turns out that I-V spectroscopy by means of conductive AFM gives us a handle on this variable. We performed such measurements on LB-films of RC-containing membrane fragments of native RCs and of the AM149W and AM260W RC-variants. At low contact force of the probe

tip the I-V curves of native RCs have a very asymmetric shape: the current is recorded only for positive applied potential, with a negligible response at negative potentials. The immediate conclusion is that electron tunneling in the RC is highly vectorial, strongly reminiscent of the light-induced electron transfer. This current response is similar to that of a diode, which supports current only in forward biased conditions. These results are similar to the ones that have been reported in the literature for Photosystem I complexes with different orientations on the surface of an electrode.<sup>16,17,19,46</sup>

The effect of increasing contact force follows the same trend as we reported in Chapter 2: the shape of the I-V curve remains roughly the same, but the magnitude of the current increases until a critical point is reached where presumably the LB layer is perforated and the tip makes direct contact with the underlying electrode. The increase of the tunneling current is probably due to a decrease of the barrier width as a result of compression of the protein complex. The amplitude of the tunneling current is roughly the same as the RC-associated component in the I-V curves of the RC-LH1 complex described in Chapter 2.

In order to further investigate the role of co factors in electron transfer in bacterial RCs, we have compared the photocurrent generated by membrane fragments containing native RCs with those containing RC-variants in which specific cofactors were missing. The photocurrents generated by adsorbed RCs and the AM149W RC-variant (with depleted H<sub>B</sub>) have very similar current the same time profile. This measurement show that H<sub>B</sub> does not have any functional role in trans-membrane electron tunneling in RCs. However, for the AM260W RC-variant (with depleted Q<sub>A</sub>)<sup>1</sup> no photocurrent was recorded, which is evidence of a vital role of Q<sub>A</sub> in trans-membrane electron transfer. From these results we surmise that the electron tunneling follows the same path as in light-induced charge separation.

---

<sup>1</sup> Q<sub>A</sub> depleted RCs of *R. sphaeroides* mutations were prepared by introducing mutations close to the Q<sub>A</sub> site. Two of them, Ala M260 to Trp and Ala M248 to Trp resulted in Q<sub>A</sub> depletion, while abolishing photosynthetic growth of the bacterium. Electron transfer from the primary donor to H<sub>A</sub> was retained,. The observations were later confirmed by X-ray crystallography data that showed exclusion of Q<sub>A</sub> from the reaction center. It was concluded from the X-ray structural data that the volume of the cavity was reduced and the site was occupied by a chloride ion.

Electron transfer from the electrode then must populate the lowest unoccupied molecular orbital (LUMO) of the special pair, from where it migrates to the quinone acceptor exclusively along the A-branch of the RC. When the  $Q_A$  site is empty, as in the AM260W RC-variant, the distance of  $H_A$  to the electrode at the cytoplasmic side is too large for electron tunneling.

Photocurrent measurements of the AM149W and AM260W RC-variants in the presence of mediators are in agreement with the I-V spectroscopy data. In the absence of  $Q_A$  electron transfer to the Q-0 pool in solution appears to be blocked. We also may conclude that under those conditions the B-branch of the RC remains inactive. This is consistent with earlier reports that no electron transfer along the B-branch is observed by only inhibiting electron transfer along the A-branch of the complex.<sup>7</sup>

The mutation of Ala M149 to Trp (AM149W) leads to the assembly of RCs without the  $H_B$  cofactor. The absence of this cofactor does neither affect the capability of the RCs to grow photosynthetically, or impair electron transfer from the special pair to  $Q_A$ . X-ray crystallography and FTIR data have confirmed the absence of  $H_B$  in the complex<sup>24</sup>. Our measurements of photocurrent with the AM149W RC support these findings because the magnitude and time profile of photocurrents recorded for adsorbed AM149W and native RCs on gold electrode are very similar, which is evidence of the fact that  $H_B$  does not have any functional importance. It may, however, have a structural importance or some other role which is not yet known.

The asymmetry of the I-V response of gold-adsorbed RC-membrane fragments is a significant result: because of vectorial electron transfer the direction of the tunneling current will depend on the orientation of the RC complex in the tunneling junction. Opposite orientations of the RC complex in the tunneling junction will thus elicit distinctly different I-V curves which should be inverted around  $V = 0$ . What we observe is that, apart from limited (up to 25%) variations in the amplitude, the I-V response from one point to the other is always very similar. This provides conclusive evidence that the large majority of the RC-membrane fragments have the same orientation. Combined with the evidence for direct electron transfer from the flat gold electrode, we conclude that the RC complexes in the LB layers have the same orientation and moreover, that the preferred

orientation corresponds to adsorption of RCs with the periplasmic side facing the gold surface.

## 6. Conclusion

Membrane fragments containing RCs, AM149W and AM260W RC-variants were deposited on a flat gold electrode by adsorption and LB-deposition. They formed dense monolayers with a high degree of orientation, with the periplasmic side of the RC complexes facing the gold surface. Direct electron transfer from the gold surface to the special pair was observed. IV spectroscopy by conductive AFM showed that electron tunneling in the RC complex follows the same path along the A-branch as light-induced charge separation.

## References

1. Kellogg, E. C.; Kolaczowski, S.; Wasielewski, M. R.; Tiede, D. M. Measurement of the Extent of Electron-Transfer to the Bacteriopheophytin in the M-Subunit in Reaction Centers of *Rhodospseudomonas-Viridis*. *Photosynthesis Research* 1989, 22 (1), 47-59.
2. Paddock, M. L.; Chang, C.; Xu, Q.; Abresch, E. C.; Axelrod, H. L.; Feher, G.; Okamura, M. Y. Quinone (Q(B)) reduction by B-branch electron transfer in mutant bacterial reaction centers from *Rhodobacter sphaeroides*: Quantum efficiency and X-ray structure. *Biochemistry* 2005, 44 (18), 6920-6928.
3. Allen, J. P.; Feher, G.; Yeates, T. O.; Komiya, H.; Rees, D. C. Structure of the Reaction Center from *Rhodobacter-Sphaeroides* R-26 - the Cofactors .1. *Proceedings of the National Academy of Sciences of the United States of America* 1987, 84 (16), 5730-5734.
4. Deisenhofer, J.; Michel, H. Structures of Bacterial Photosynthetic Reaction Centers. *Annual Review of Cell Biology* 1991, 7, 1-23.
5. Nogi, T.; Miki, K. Structural basis of bacterial photosynthetic reaction centers. *Journal of Biochemistry* 2001, 130 (3), 319-329.
6. de Boer, A. L.; Neerken, S.; de Wijn, R.; Permentier, H. P.; Gast, P.; Vijgenboom, E.; Hoff, A. J. High yield of B-branch electron transfer in a quadruple reaction center mutant of the photosynthetic bacterium *Rhodobacter sphaeroides*. *Biochemistry* 2002, 41 (9), 3081-3088.
7. de Boer, A. L.; Neerken, S.; de Wijn, R.; Permentier, H. P.; Gast, P.; Vijgenboom, E.; Hoff, A. J. B-branch electron transfer in reaction centers of *Rhodobacter sphaeroides* assessed with site-directed mutagenesis. *Photosynthesis Research* 2002, 71 (3), 221-239.
8. Frolov, D.; Wakeham, M. C.; Andrizhiyevskaya, E. G.; Jones, M. R.; van, G. R. Investigation of B-branch electron transfer by femtosecond time resolved spectroscopy in a *Rhodobacter sphaeroides* reaction centre that lacks the Q(A) ubiquinone. *Biochim. Biophys. Acta* 2005, 1707 (2-3), 189-198.

9. Haffa, A. L. M.; Lin, S.; Williams, J. C.; Bowen, B. P.; Taguchi, A. K. W.; Allen, J. P.; Woodbury, N. W. Controlling the pathway of photosynthetic charge separation in bacterial reaction centers. *Journal of Physical Chemistry B* 2004, 108 (1), 4-7.
10. Hartwich, G.; Bieser, G.; Langenbacher, T.; Muller, P.; Richter, M.; Ogrodnik, A.; Scheer, H.; MichelBeyerle, M. E. B-branch electron transfer in bacterial photosynthetic reaction centers by energetically activating A-branch charge separation. *Biophysical Journal* 1997, 72 (2).
11. Kirmaier, C.; Laible, P. D.; Hanson, D. K.; Holten, D. B-side charge separation in bacterial photosynthetic reaction centers: Nanosecond time scale electron transfer from H-B(-) to Q(B). *Biochemistry* 2003, 42 (7), 2016-2024.
12. Laible, P. D.; Kirmaier, C.; Udawatte, C. S. M.; Hofman, S. J.; Holten, D.; Hanson, D. K. Quinone reduction via secondary B-branch electron transfer in mutant bacterial reaction centers. *Biochemistry* 2003, 42 (6), 1718-1730.
13. Marchanka, A.; Savitsky, A.; Lubitz, W.; Mobius, K.; van Gestel, M. B-Branch Electron Transfer in the Photosynthetic Reaction Center of a Rhodobacter sphaeroides Quadruple Mutant Q- and W-Band Electron Paramagnetic Resonance Studies of Triplet and Radical-Pair Cofactor States. *Journal of Physical Chemistry B* 2010, 114 (45), 14364-14372.
14. Davis, J. J.; Morgan, D. A.; Wrathmell, C. L.; Axford, D. N.; Zhao, J.; Wang, N. Molecular bioelectronics. *Journal of Materials Chemistry* 2005, 15 (22), 2160-2174.
15. Kondo, M.; Iida, K.; Dewa, T.; Tanaka, H.; Ogawa, T.; Nagashima, S.; Nagashima, K. V. P.; Shimada, K.; Hashimoto, H.; Gardiner, A. T.; Cogdell, R. J.; Nango, M. Photocurrent and Electronic Activities of Oriented-His-Tagged Photosynthetic Light-Harvesting/Reaction Center Core Complexes Assembled onto a Gold Electrode. *Biomacromolecules* 2012, 13 (2), 432-438.
16. Mikayama, T.; Miyashita, T.; Iida, K.; Suemori, Y.; Nango, M. Electron transfer mediated by photosynthetic reaction center proteins between two chemical-modified metal electrodes. *Molecular Crystals and Liquid Crystals* 2006, 445, 291-296.
17. Reiss, B. D.; Hanson, D. K.; Firestone, M. A. Evaluation of the photosynthetic reaction center protein for potential use as a bioelectronic circuit element. *Biotechnology Progress* 2007, 23 (4), 985-989.
18. Song, H.; Lee, H.; Lee, T. Characterization of the tip-loading force-dependent tunneling behavior in alkanethiol metal-molecule-metal junctions by conducting atomic force microscopy. *Ultramicroscopy* 2008, 108 (10), 1196-1199.
19. Stamouli, A.; Frenken, J. W. M.; Oosterkamp, T. H.; Cogdell, R. J.; Aartsma, T. J. The electron conduction of photosynthetic protein complexes embedded in a membrane. *Febs Letters* 2004, 560 (1-3), 109-114.
20. Xi, W.; Zhang, W.; An, B. K.; Burn, P. L.; Davis, J. J. Tunneling conductance of vectorial porphyrin monolayers. *Journal of Materials Chemistry* 2008, 18 (26), 3109-3120.
21. McAuley, K. E.; Fyfe, P. K.; Ridge, J. P.; Cogdell, R. J.; Isaacs, N. W.; Jones, M. R. Ubiquinone binding, ubiquinone exclusion, and detailed cofactor conformation in a mutant bacterial reaction center. *Biochemistry* 2000, 39 (49), 15032-15043.
22. Ridge, J. P.; van Brederode, M. E.; Goodwin, M. G.; van Grondelle, R.; Jones, M. R. Mutations that modify or exclude binding of the QA ubiquinone and carotenoid in the reaction center from Rhodobacter sphaeroides. *Photosynthesis Research* 1999, 59 (1), 9-26.

23. Wakeham, M. C.; Goodwin, M. G.; McKibbin, C.; Jones, M. R. Photo-accumulation of the P+QB- radical pair state in purple bacterial reaction centres that lack the QA ubiquinone. *FEBS Lett.* 2003, 540 (1-3), 234-240.
24. Watson, A. J.; Fyfe, P. K.; Frolov, D.; Wakeham, M. C.; Nabedryk, E.; Van Grondelle, R.; Breton, J.; Jones, M. R. Replacement or exclusion of the B-branch bacteriopheophytin in the purple bacterial reaction centre: The H-B cofactor is not required for assembly or core function of the *Rhodobacter sphaeroides* complex. *Biochimica et Biophysica Acta-Bioenergetics* 2005, 1710 (1), 34-46.
25. Jones, M. R.; Heerdawson, M.; Mattioli, T. A.; Hunter, C. N.; Robert, B. Site-Specific Mutagenesis of the Reaction-Center from *Rhodobacter-Sphaeroides* Studied by Fourier-Transform Raman-Spectroscopy - Mutations at Tyrosine M210 do Not Affect the Electronic-Structure of the Primary Donor. *Febs Letters* 1994, 339 (1-2), 18-24.
26. Wakeham, M. C.; Breton, J.; Nabedryk, E.; Jones, M. R. Formation of a semiquinone at the QB site by A- or B-branch electron transfer in the reaction center from *Rhodobacter sphaeroides*. *Biochemistry* 2004, 43 (16), 4755-4763.
27. van Baarle, G. J. C.; Troianovski, A. M.; Nishizaki, T.; Kes, P. H.; Aarts, J. Imaging of vortex configurations in thin films by scanning-tunneling microscopy. *Applied Physics Letters* 2003, 82 (7), 1081-1083.
28. Straley, S. C.; Parson, W. W.; MAUZERAL.DC; Clayton, R. K. Pigment Content and Molar Extinction Coefficients of Photochemical Reaction Centers from *Rhodospseudomonas-Sphaeroides*. *Biochimica et Biophysica Acta* 1973, 305 (3), 597-609.
29. Semchonok, D. A.; Chauvin, J. P.; Frese, R. N.; Jungas, C.; Boekema, E. J. Structure of the dimeric RC-LH1-PufX complex from *Rhodobaca bogoriensis* investigated by electron microscopy. *Philosophical Transactions of the Royal Society B-Biological Sciences* 2012, 367 (1608), 3412-3419.
30. Alegria, G.; Dutton, P. L. Langmuir-Blodgett Monolayer Films of Bacterial Photosynthetic Membranes and Isolated Reaction Centers - Preparation, Spectrophotometric and Electrochemical Characterization .1. *Biochimica et Biophysica Acta* 1991, 1057 (2), 239-257.
31. Lu, Y.; Xu, J.; Liu, B.; Kong, J. Photosynthetic reaction center functionalized nano-composite films: effective strategies for probing and exploiting the photo-induced electron transfer of photosensitive membrane protein. *Biosens. Bioelectron.* 2007, 22 (7), 1173-1185.
32. Yasuda, Y.; Hirata, Y.; Sugino, H.; Kumei, M.; Hara, M.; Miyake, J.; Fujihira, M. Langmuir-Blodgett-Films of Reaction Centers of *Rhodospseudomonas-Viridis* - Photoelectric Characteristics. *Thin Solid Films* 1992, 210 (1-2), 733-735.
33. Yasuda, Y.; Sugino, H.; Toyotama, H.; Hirata, Y.; Hara, M.; Miyake, J. Control of Protein Orientation in Molecular Photoelectric Devices Using Langmuir-Blodgett-Films of Photosynthetic Reaction Centers from *Rhodospseudomonas-Viridis*. *Bioelectrochemistry and Bioenergetics* 1994, 34 (2), 135-139.
34. Zaitsev, S. Y.; Kalabina, N. A.; Zubov, V. P.; Lukashev, E. P.; Kononenko, A. A.; Uphaus, R. A. Monolayers of Photosynthetic Reaction Centers of Green and Purple Bacteria. *Thin Solid Films* 1992, 210 (1-2), 723-725.
35. Lu, Y. D.; Xu, J. J.; Liu, B. H.; Kong, J. L. Photosynthetic reaction center functionalized nano-composite films: Effective strategies for probing and exploiting the photo-induced electron transfer of photosensitive membrane protein. *Biosensors & Bioelectronics* 2007, 22 (7), 1173-1185.

36. Lukashev, E. P.; Nadtochenko, V. A.; Permenova, E. P.; Sarkisov, O. M.; Rubin, A. B. Electron phototransfer between photosynthetic reaction centers of the bacteria *Rhodobacter sphaeroides* and semiconductor mesoporous TiO<sub>2</sub> films. *Doklady Biochemistry and Biophysics* 2007, 415 (1), 211-216.
37. Nakamura, C.; Hasegawa, M.; Yasuda, Y.; Miyake, J. Self-assembling photosynthetic reaction centers on electrodes for current generation. *Applied Biochemistry and Biotechnology* 2000, 84-6, 401-408.
38. Trammell, S. A.; Wang, L. Y.; Zullo, J. M.; Shashidhar, R.; Lebedev, N. Orientated binding of photosynthetic reaction centers on gold using Ni-NTA self-assembled monolayers. *Biosensors & Bioelectronics* 2004, 19 (12), 1649-1655.
39. Trammell, S. A.; Spano, A.; Price, R.; Lebedev, N. Effect of protein orientation on electron transfer between photosynthetic reaction centers and carbon electrodes. *Biosensors & Bioelectronics* 2006, 21 (7), 1023-1028.
40. Trammell, S. A.; Griva, I.; Spano, A.; Tsoi, S.; Tender, L. M.; Schnur, J.; Lebedev, N. Effects of distance and driving force on photoinduced electron transfer between photosynthetic reaction centers and gold electrodes. *Journal of Physical Chemistry C* 2007, 111 (45), 17122-17130.
41. Ueno, T.; Hara, M.; Kamo, N.; Fujii, T.; Miyake, J. Control of the unidirectional topological orientation of a cross-linked complex composed of the bacterial photosynthetic reaction center and horse heart cytochrome c reconstituted into proteoliposomes. *Journal of Biochemistry* 1998, 124 (3), 485-490.
42. den Hollander, M. J.; Magis, J. G.; Fuchsenberger, P.; Aartsma, T. J.; Jones, M. R.; Frese, R. N. Enhanced Photocurrent Generation by Photosynthetic Bacterial Reaction Centers through Molecular Relays, Light-Harvesting Complexes, and Direct Protein-Gold Interactions. *Langmuir* 2011, 27 (16), 10282-10294.
43. Lebedev, N.; Trammell, S. A.; Spano, A.; Lukashev, E.; Griva, I.; Schnur, J. Conductive wiring of immobilized photosynthetic reaction center to electrode by cytochrome c. *Journal of the American Chemical Society* 2006, 128 (37), 12044-12045.
44. Leopold, M. C.; Bowden, E. F. Influence of gold substrate topography on the voltammetry of cytochrome c adsorbed on carboxylic acid terminated self-assembled monolayers. *Langmuir* 2002, 18 (6), 2239-2245.
45. Zhu, Z. Y.; Gunner, M. R. Energetics of quinone-dependent electron and proton transfers in *Rhodobacter sphaeroides* photosynthetic reaction centers. *Biochemistry* 2005, 44 (1), 82-96.
46. Lee, I.; Lee, J. W.; Greenbaum, E. Biomolecular electronics: Vectorial arrays of photosynthetic reaction centers. *Physical Review Letters* 1997, 79 (17), 3294-3297.